Journal of Physics: Conference Series **3124** (2025) 012012 doi:10.1088/1742-6596/3124/1/012012

Experimental characterization of the timing-jitter effects on a beam-driven plasma wakefield accelerator

F. Demurtas[1], M. P. Anania[1], A. Biagioni[1], E. Chiadroni[2], A. Cianchi[3], G. Costa[1], L. Crincoli[1], A. Del Dotto[1], M. Del Giorno[1], M. Ferrario[1], M. Galletti[1], L. Giannessi[1], A. Giribono[1], R. Pompili[1], S. Romeo[1], A. R. Rossi[4], V. Shpakov, G. J. Silvi[1], C. Vaccarezza[1], F. Villa[1]

[1] Frascati National Laboratories INFN-LNF, 00044 Frascati (RM), Italy
[2] INFN-Sez. Roma1, Rome, Italy
[3] University of Rome 'Tor Vergata', Via della Ricerca Scientifica 1, I-00133 Rome, Italy
[4] INFN-Sez Milano, 20133 Milano, Italy

E-mail: `francesco.demurtas@lnf.infn.it`

Abstract. Plasma wakefield acceleration is nowadays very attractive in terms of accelerating gradient, able to overcome conventional accelerators by orders of magnitude. However, this poses very demanding requirements on the accelerator stability to avoid large instabilities on the final beam energy. In this study we analyze the correlation between the driver-witness distance jitter (due to the radio-frequency timing jitter) and the witness energy gain in a plasma wakefied accelerator stage. Experimental measurements are reported by using an electro-optical sampling diagnostics with which we correlate the distance between the driver and witness beams before the plasma accelerator stage. The results show a clear correlation due to such a distance jitter, highlighting the contribution coming from the radio-frequency (RF) compression.

1. Introduction

Plasma Wakefield Acceleration is very important in accelerator physics to overcome the current limit of accelerating gradient in radio-frequency accelerators, in which the electric breakdown phenomenon limits the electric field to a few tens of MV/m. In plasma accelerators, the medium is already ionized so that the breakdown cannot occur, being able to reach accelerating gradients of GV/m. The acceleration mechanism is based on the excitation of a plasma wave, that is, a perturbation of the plasma density, with a driver which can be either a laser pulse (LWFA) or an electron beam (PWFA).

In plasma wakefield acceleration (PWFA), the wake is driven by the coulomb force due to the space charge effect of a relativistic charge bunch, termed driver, sent into the plasma, which creates an electron-depleted region, in which the separation between plasma-ions and electrons creates a strong accelerating electric field. Placed into the correct phase of this plasma wakefield, a short electron beam, termed the witness beam, can be accelerated up to GeV energies over centimetre distances [1].

The importance of plasma acceleration extends across many applications, such as new generation radiation sources like plasma-based Free electron laser, imposing stringent requirements on the beam quality [2].

The experiment has been performed at the SPARC_LAB facility, at the INFN-LNF, where two beams with different charges are produced with the laser-comb technique [3] to perform beam-driven plasma acceleration. At low energy, the beam dynamics is dominated by space charge forces. Therefore, the beams cannot be generated at ultra-short durations necessary for beam-driven plasma (in the order of tens of femtoseconds). The compression is achieved with velocity bunching, by injection of a chirped beam into the zero-crossing phase of the first accelerating section. Due to the velocity difference within the bunch, it will slip in phase towards higher accelerating gradients, and it is simultaneously accelerated and compressed [4].
However, this links their positions to the timing of the RF system, introducing a jitter in the separation between the bunches.
In this work, measurements are reported to evaluate the effect of the RF timing jitter on the acceleration, which is a source of a measurable jitter in the energy of the witness beam in a beam-driven plasma accelerator. The article also focuses on the diagnostics used to measure the distance between the driver and witness beams, i.e. the electro-optical sampling (EOS). The EOS is a non-intercepting and single-shot diagnostics based on the change of refracting index in an electro-optical crystal induced by the external field of the beam. This system has a resolution of a few tens of femtoseconds, being able to measure the timing jitter effect in the distance between the driver and witness beams.
The article is organized as follows: Section 2 describes the theoretical background of the experiment; the experimental setup and the description of the EOS diagnostics are presented in Section 3; finally, the measurements and analysis results are reported in Section 4.

2. Velocity bunching and arrival timing jitter

The velocity bunching is based on a longitudinal phase space rotation due to an initial difference in velocity between the bunch head and tail. The beam is injected into the RF cavity at the zero-crossing phase, as shown in figure 1, with a velocity smaller than the phase velocity of the RF travelling wave and an initial chirp in velocity, where the head has a larger velocity with respect to the tail. The bunch will slip back in phase towards a higher accelerating field: the head of the bunch will feel a smaller field with respect to the tail, and then, the bunch will be compressed and chirped simultaneously [5]. The compression with velocity bunching links the jitter in the beam's position to the RF system's timing jitter, which affects the longitudinal beam dynamics. The beam arrival timing jitter (ATJ) is influenced by two main contributions: the changing of the laser arrival time at the photocathode and the instabilities in the timing of the RF system. Other contributions, like fluctuations in the magnetic fields and the RF system amplitude, are negligible). Therefore, the primary ATJ sources are the laser photocathode and the two S-band klystron named K1 and K2, in which the first feeds the gun and the third linac section called S3, while K2 feeds the two first sections S1 (used for beam compression) and S2. The beam arrival time variation is given by the sum of all contributions:

$$\Delta t_{linac} \simeq \sum_{i=1}^{3} c_i \Delta t_i \tag{1}$$

where i=1 refers to the laser photocathode, i=2 and i=3 refer respectively to K1 and K2. After the linac exit the coefficient c_3 related to the S1 fields is much larger than c_1 and c_2, being the leading contribution to the beam arrival timing jitter [6]. The ATJ in the relative distance between the driver and witness results in a jitter in the witness energy when accelerated in plasma. The driver excites a wakefield with a slope depending on the plasma density. Since the witness is jittering in position along the wakefield, it will feel a different accelerating gradient and result in different energy gains.

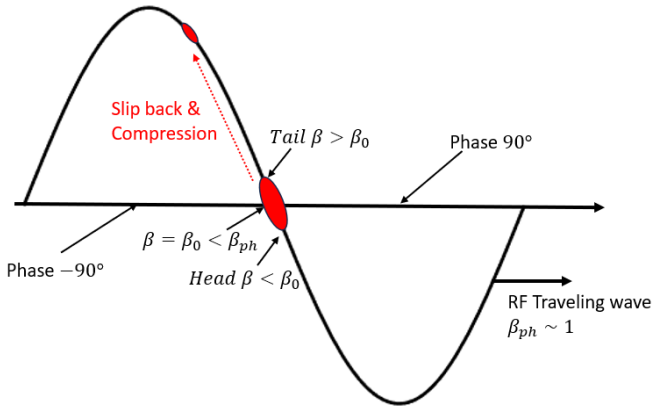

Figure 1. Velocity bunching slippage on the RF wave: since the bunch velocity is smaller than the wave's phase velocity and there is a velocity chirp, it will slip in phase towards higher accelerating fields and be compressed.

3. Experimental Setup

The experimental setup at the SPARC LAB test facility is shown in figure 2. Two bunches of different charges, driver and witness, are produced with the laser-comb technique [8] at the SPARC photo-injector, consisting of an RF gun which accelerates the beams up to $\sim 5MeV$. The gun is followed by three S-Band accelerating sections, in which the first acts as a compressor. Since the compression is done at low energy, a solenoid around the gun will allow for the necessary emittance compensation process to avoid emittance growth due to space charge effects.

The witness beam is accelerated with a plasma accelerator consisting of a discharge capillary, shown in figure 3, of 3 cm length and 1 mm diameter, filled with Hydrogen, in which the driver excites a plasma wakefield capable of accelerating the witness. The measured plasma density is $n_e e \sim 10^{15} - 10^{16}\ cm^{-3}$.

The beam diagnostics consists of the electro-optical sampling before the plasma accelerator and a magnetic spectrometer after the plasma, allowing for the beam longitudinal characterization with two Ce:YAG (Cerium-Doped Yttrium Aluminium Garnet) scintillator screens.

The plasma has been stabilized with a laser pulse; therefore, the timing-jitter effect on the bunches is due mainly to the RF instabilities [9].

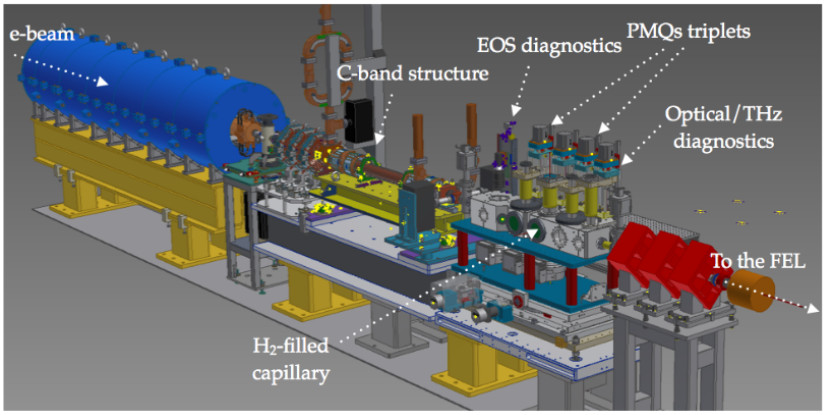

Figure 2. Layout of the experimental setup, in which are highlighted the EOS diagnostics, the plasma capillary and the optical components of the line [10].

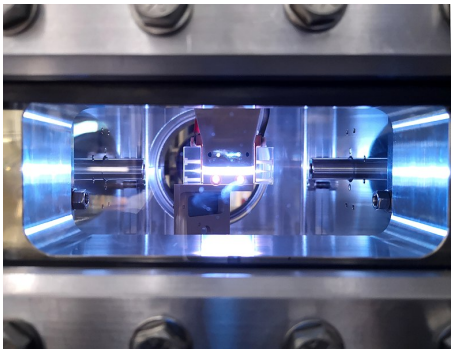

Figure 3. Picture of the plasma discharge-capillary; the capillary is 3 cm long, and with a 1 mm diameter, it is filled with Hydrogen at a plasma density of $10^{15} - 10^{16}\ cm^{-3}$ [11]

3.1. Electro-Optical Sampling

The Electro-Optical Sampling is a non-intercepting and single-shot device used to measure the beam longitudinal properties, and in this case the distance between driver and witness. The working principle is based on an external field, i.e. the beam coulomb field, which induces birefringence on an electro-optical crystal. The crystal used in the experiment is zinc telluride (ZnTe).

A slowly varying external electric field $E_{ext}(t)$ (with a frequency in the THz region) induces a change in the refractive indexes in the crystal, which follows the temporal profile of the field.

The change in refractive index can be measured with an opportune polarized laser pulse that crosses the crystal. This effect produces a phase delay $\Gamma(t)$ between the laser horizontal and vertical components, which is proportional to the beam electric field. The detected intensity is given by:

$$I_{det} = I_{laser}^2 sin^2\Gamma \tag{2}$$

where the phase delay $\Gamma(t) = \frac{\pi d}{\lambda} n_0^3 r_{41} E_{ext}(t)$ depends on the external electric field $E_{ext}(t)$ induced by the beam, the non-linear coefficient r_{41}, the laser wavelength λ, the crystal thickness d, and unperturbed refractive index n_0.

The Electro-optical sampling can be implemented in various configurations, depending on the experimental needs. The main configurations are spectral decoding, in which the laser probe propagates parallel to the electron beam [12], temporal and spatial decoding, in which the probe is transverse to the beam [13], and also the recently proposed "diversity electro-optical sampling" (DEOS) [14].

In this experiment, the EOS has been implemented in the spatial decoding scheme in which the laser crosses the crystal with an angle $\theta = 30\ deg$ with respect to the beam propagation axis, as shown in figure 4 [15]. The beam passes close to the crystal and produces an external field which modifies the crystal's properties. Different points across the transverse profile of the probe beam pass through the crystal at different times and experience the external field at different instances in time, acquiring a different polarization.

The time coordinate t is related to the spatial coordinate x through the formula:

$$t = \frac{x}{c} tan\theta \tag{3}$$

The field temporal profile is imprinted on the transverse spatial variation of the probe beam, allowing for retrieving the electron beam longitudinal information [16].

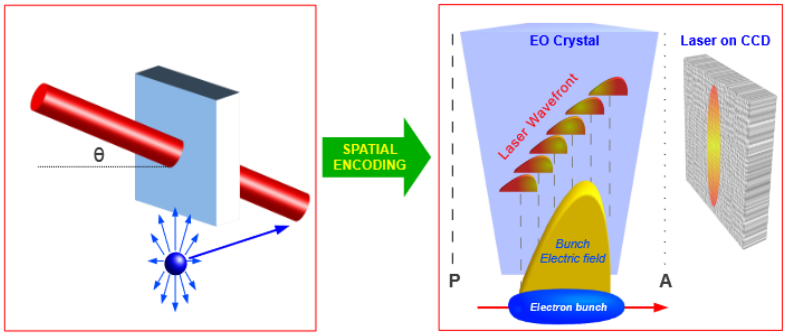

Figure 4. Working principle of the EOS spatial decoding configuration: the laser pulse crosses the crystal with an angle $\theta = 30\ deg$ and therefore different points on the pulse front wave feel a different external field and acquire a different polarization; then by the recorded laser pulse it is possible to reconstruct the beam longitudinal distribution [15].

4. Measurement and Analysis results

The measurements of the witness energy have been taken at the magnetic spectrometer after the plasma accelerator, and the distance between the bunches has been measured with the EOS before the plasma. The pictures taken from the two cameras are shown in figure 5 and 6, in which the signal is composed by the superposition of all the taken shots.

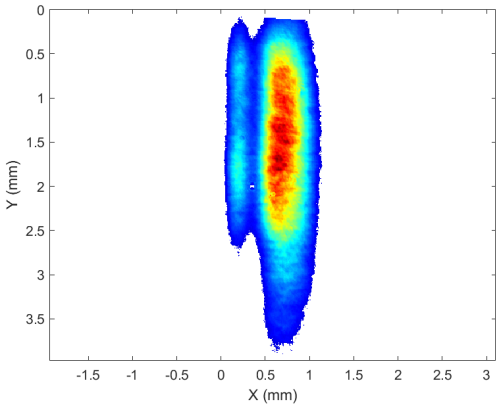

Figure 5. Bunch measurement with the EOS system, the image is obtained by summing the signal of all the taken pictures.

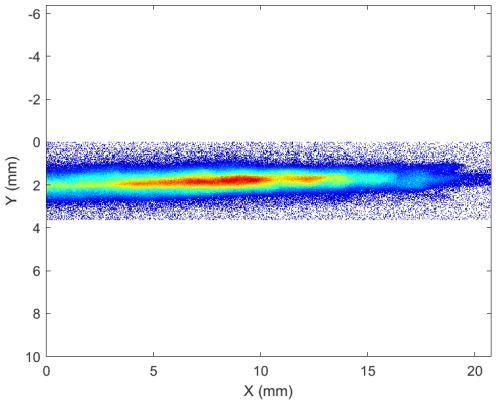

Figure 6. Energy measurement of the witness beam after the spectrometer, the image is obtained by summing the signal of all the taken pictures.

The driver beam has charge $Q_D = (200 \pm 5)\ pC$, while the witness is $Q_D = (20 \pm 3)\ pC$. After the linac, the witness beam has an energy $E \sim 87\ MeV$ with a spread $\Delta E \sim 0.45\ MeV$. Considering 400 consecutive shots, after the acceleration in plasma, the measured mean energy is $E_{mean} = (92.3 \pm 0.4)\ MeV$ with a corresponding energy spread of $E_{spread} = (0.4 \pm 0.1)\ MeV$, resulting in an acceleration of about $\Delta E = 5\ MeV$. The measured average distance between the bunches is $\Delta t = (1.03 \pm 0.06)\ ps$. The measurements highlighted a linear correlation between the measured jitters as shown in figure 7, with an angular coefficient $m_{fit} = (10 \pm 1)\ keV/fs$.

Since the wakefield slope is large because of the large accelerating field in the plasma, the jitter effect in the acceleration is appreciable [17]. All the results are shown in table 1.

Table 1. Results of the measurement. E_{mean} is the witness mean energy, E_{spread} is the witness energy spread, Δt is the average distance between the beams and m_{fit} is the angular coefficient of the linear fit.

Beam Parameters	Value	Unit
E_{mean}	92.3 ± 0.4	MeV
E_{spread}	0.4 ± 0.1	MeV
Δt	1.03 ± 0.06	ps
m_{fit}	10 ± 1	keV/fs

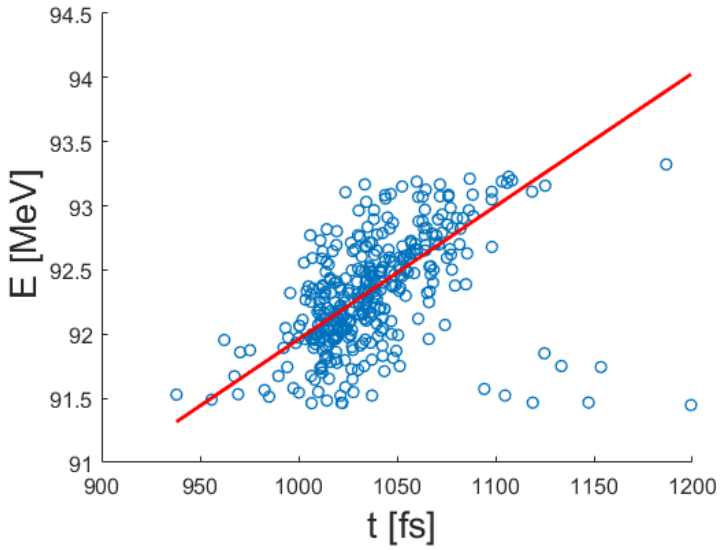

Figure 7. Measurement with the corresponding linear fit of the correlation between the distance driver-witness and the witness energy after the plasma; the fit has angular coefficient $m = (10 \pm 1)$ keV/fs.

5. Conclusion and outlook

This paper has discussed the effect of the RF timing jitter in a plasma wakefield accelerator. The electro-optical sampling allowed us to measure a jitter in the order of a few tens of femtoseconds. The results showed a linear correlation between the relative jitter in the distance driver-witness and the witness energy jitter. These measurements can be instrumental in characterizing the stability of a plasma accelerator with different plasma modules, i.e. a different type of plasma capillary. The presented study will be updated with further measurements at SPARC and supported with simulation from the tracking code Astra [18].

Reference

[1] Gschwendtner, Edda, and Patric Muggli. "Plasma wakefield accelerators." Nature Reviews Physics 1.4 (2019): 246-248.
[2] D'Arcy, Richard, et al. "FLASHForward: plasma wakefield accelerator science for high-average-power applications." Philosophical Transactions of the Royal Society A 377.2151 (2019): 20180392.
[3] Chiadroni, Enrica, et al. "Status of plasma-based experiments at the SPARC_LAB test facility." 9th Int. Particle Accelerator Conf.(IPAC'18), Vancouver, Canada. 2018.
[4] Filippetto, D., et al. "Velocity bunching experiment at SPARC." Proc. of the FEL 2009 conference, Liverpool, UK. 2009.
[5] Serafini, L., and M. Ferrario. "Velocity bunching in photo-injectors." AIP conference proceedings. Vol. 581. No. 1. American Institute of Physics, 2001.
[6] Pompili, Riccardo, et al. "Femtosecond timing-jitter between photo-cathode laser and ultra-short electron bunches by means of hybrid compression." New Journal of Physics 18.8 (2016): 083033.
[7] Alesini, D., et al. "The SPARC project: a high-brightness electron beam source at LNF to drive a SASE-FEL experiment." Nuclear Instruments and Methods in Physics Research Section A: Accelerators, Spectrometers, Detectors and Associated Equipment 507.1-2 (2003): 345-349.
[8] Ferrario, M., et al. "Laser comb with velocity bunching: Preliminary results at SPARC." Nuclear Instruments and Methods in Physics Research Section A: Accelerators, Spectrometers, Detectors and Associated Equipment 637.1 (2011): S43-S46.
[9] Biagioni, Angelo, et al., Plasma Physics and Controlled Fusion 63.11 (2021): 115013.
[10] Chiadroni, Enrica, et al. "Status of plasma-based experiments at the SPARC_LAB test facility." 9th Int. Particle Accelerator Conf.(IPAC'18), Vancouver, Canada. 2018.
[11] Pompili, Riccardo, et al. "Energy spread minimization in a beam-driven plasma wakefield accelerator." Nature Physics 17.4 (2021): 499-503.
[12] Jamison, S. P., et al. "Electro-optic techniques for temporal profile characterisation of relativistic Coulomb fields and coherent synchrotron radiation." Nuclear Instruments and Methods in Physics Research Section A: Accelerators, Spectrometers, Detectors and Associated Equipment 557.1 (2006): 305-308.
[13] Parc, Yong Woon, and In Soo Ko. "Analysis of the electro-optic measurement of an electron beam with new refractive indices." Journal of Optics A: Pure and Applied Optics 11.10 (2009): 105704.
[14] Roussel, Eléonore, et al. "Phase Diversity Electro-optic Sampling: A new approach to single-shot terahertz waveform recording." Light: Science & Applications 11.1 (2022): 14.
[15] Pompili, R., et al. "First single-shot and non-intercepting longitudinal bunch diagnostics for comb-like beam by means of electro-optic sampling." Nuclear Instruments and Methods in Physics Research Section A: Accelerators, Spectrometers, Detectors and Associated Equipment 740 (2014): 216-221.
[16] R. Pompili, PhD Thesis at SPARC_LAB. Longitudinal diagnostics for comb-like electron beams by means of Electro-Optic Sampling (2013).
[17] F. Demurtas, et al. "Experimental characterization of the timing-jitter effects on a beam-driven plasma wakefield accelerator". Poster presented at "6th European Advanced Accelerator Concepts Workshop", Isola d'Elba, Italy (2023).
[18] Flottmann, Klaus, Steven Lidia, and Philippe Piot. Recent improvements to the ASTRA particle tracking code. No. LBNL-52933. Lawrence Berkeley National Lab.(LBNL), Berkeley, CA (United States), 2003.